

Supporting Information

Metallic phase WSe₂ nanoscrolls for hydrogen evolution reaction

Wei Wang¹, Yutong Li¹, Mengjia Li¹, Hailin Shen¹, Wei Zhang¹, Jintao Zhang¹, Tianyu Liu^{1,*}, Xianqiang Kong^{1,*},
Hengchang Bi^{2,*}

¹ School of Chemical Engineering and Materials, Changzhou Institute of Technology, Changzhou 213032, P.R. China,

² Shanghai Key Laboratory of Multidimensional Information Processing, School of Communication and Electronic Engineering, East China Normal University, Shanghai 200241, P.R. China

* Corresponding author (E-mail addresses: liuty@czu.cn (Tianyu Liu); kongxq@czu.cn (Xianqiang Kong); hcbi@cee.ecnu.edu.cn (Hengchang Bi))

Experimental section

Synthesis of the M-WSe₂ nanoscrolls

The bulk WSe₂ crystals were put into an agate mortar and ground for about 30 min. After grinding in the agate mortar, the bulk WSe₂ powders were collected. The n-butyllithium solution (2 mL, 1.6 M in hexane) was mixed with the bulk WSe₂ powders (100 mg) and let it still for about 72 h. Then, the Li-intercalated WSe₂ samples were washed with n-hexane three times. Then, the samples were transferred to 40 ml DI water and sonicated for about 30 min. The unexfoliated bulk WSe₂ powders were removed by centrifuging the obtained solution at 1000 r.p.m for 10 min. Then, the obtained suspension was centrifuged at 10,000 r.p.m for another 10 min. The resulting M-WSe₂ nanosheets precipitate was re-dispersed in ethanol (0.1 mg mL⁻¹), then let stand for about 72 h. Finally, the spontaneous curled M-WSe₂ nanoscrolls were obtained after centrifuging at 10,000 r.p.m. for 15 min, and re-dispersed in ethanol before usage and characterization. For comparison, 2H WSe₂ nanoscrolls were prepared by a thermal annealing method similar to the previous reported work.[1] First, the M-WSe₂ nanoscrolls dispersion liquid was centrifuged and moved to the vial, and dried in a vacuum drying oven for about 24 h. Then after thermal annealing at 200 °C for 4 h in N₂ the 2H WSe₂ nanoscrolls were obtained.

Characterization

The field-emission scanning electron microscope (Nova NanoSEM450, FEI, USA) coupled with energy dispersive X-ray spectroscopy (EDX) was used to record scanning electron microscope (SEM) images and EDX spectrum. The crystal structure of the sample was investigated by X-ray diffraction (XRD) on a Rigaku Smartlab 3 kW using CuK α 1 radiation (Johansson-type monochromator) and a 1D detector (D/Tex Ultra) in a 2 θ range of 10°-80°. The FEI Titan 80-300 instrument was used to record the transmission electron microscopy (TEM) images. The VG ESCALAB 220i-XL spectrometer equipped with a monochromatic Al K α (1486.7 eV) X-ray source was used to collect the X-ray photoelectron spectroscopy (XPS) data. The WITec system (Germany) using a 532 nm laser excitation with a power of < 0.1 mW was used to investigate the Raman data. The UV-visible spectrophotometer (UV-2700, Shimadzu, Japan) was used to collect the UV-vis absorption spectra at room temperature.

Electrochemical measurements

All electrochemical measurements were conducted in the standard three-electrode system using a CHI electrochemical workstation (760E) at room temperature. A 0.5 M H₂SO₄ aqueous solution was employed as the electrolyte. The Ag/AgCl (3 M KCl) and Pt wire were used as the reference electrode and counter electrode, respectively. And the Ag/AgCl electrode was calibrated using a reversible hydrogen electrode (RHE) as reference (Figure S9). The working electrode was prepared by dropping an appropriate amount of the catalyst ink onto a pre-polished glassy carbon (GC) electrode (3 mm in diameter). Inks were fabricated by ultrasonically dispersing 1 mg of the M-WSe₂ nanoscrolls in a suspension containing 1 mg of carbon black, 970 μ L of isopropanol, 30 μ L of a Nafion (5 wt%) solution. The loading amount of M-WSe₂ nanoscrolls was about 24 μ g. All the linear sweep voltammograms (LSV) were measured at a scanning rate of 10 mV s⁻¹. Electrochemical impedance spectroscopy (EIS) was measured at the frequency from 0.1 to 100,000 Hz with an amplitude of 10 mV. As a reference, the commercial Pt/C catalyst was also tested.

To assess the electrochemical active surface area (ECSA) through the electrochemical double-layer capacitance (C_{dl}, mF cm⁻²) measurement, cyclic voltammograms (CV) of M-WSe₂ nanoscrolls and 2H WSe₂ nanoscrolls were measured in a non-Faradaic region between 0.220 to 0.720 V (versus RHE) in the N₂-saturated 0.5 M H₂SO₄ aqueous solution at seven different scan rates (10, 20, 50, 100, 200, 400, and 800 mV s⁻¹).

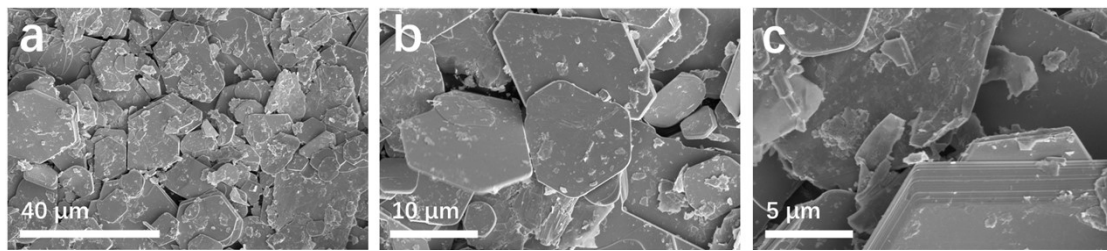


Figure S1. (a-c) SEM images of bulk WSe₂.

The chemical composition of the bulk WSe₂ precursors has been analyzed by elements mapping and energy dispersive X-ray (EDX) (Figure S2, Figure S3). The STEM image of bulk WSe₂ precursors is displayed in Figure S2a. Figure S2b and S2c show the corresponding elemental mapping results, exhibiting the W and Se elements are distributed homogenously in the plate-like WSe₂ precursors. The EDX results suggest the existence of W and Se elements in the bulk WSe₂ precursors, consisting well with the element mapping results (Figure S3).

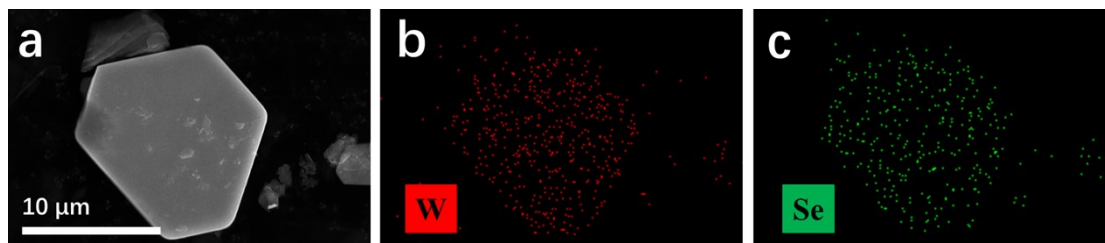


Figure S2. (a-c) elemental mapping of bulk WSe₂ the by STEM. a: STEM image of bulk WSe₂; b,c: the images of tungsten, and selenium elements.

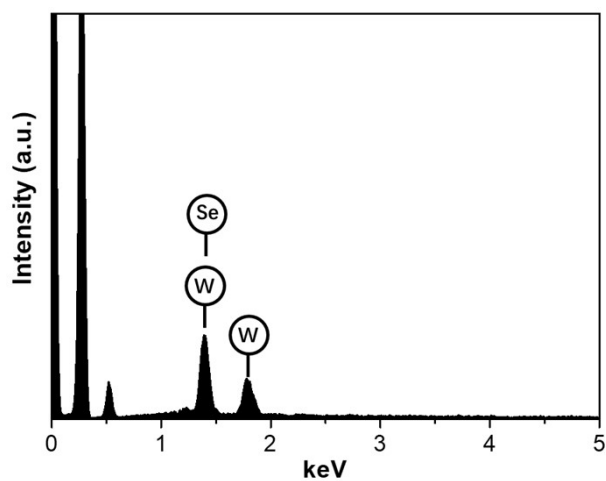


Figure S3. EDX spectrum of bulk WSe₂ powders.

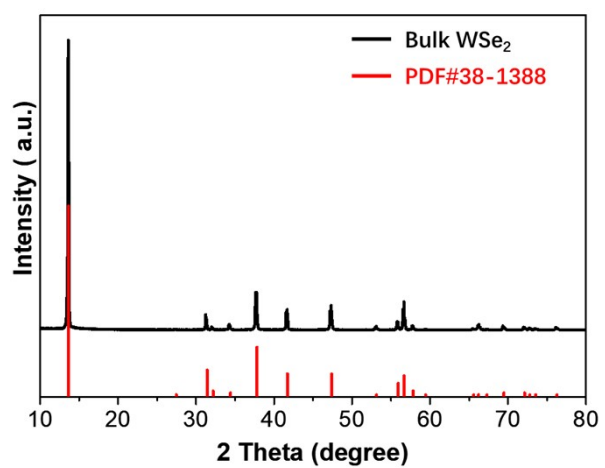


Figure S4. XRD of bulk WSe₂ powders.

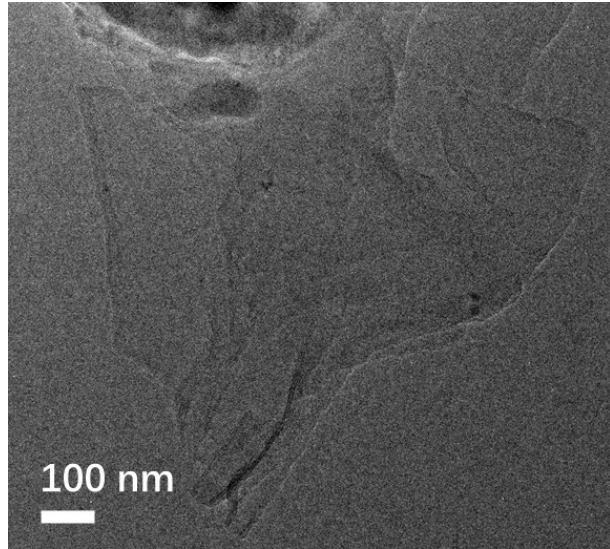


Figure S5. TEM images of M-WSe₂ nanosheets.

Figure S6 show the TEM images of 2H-WSe₂ nanoscrolls. As shown in Figure S6, the obtained samples still display the hollow scroll-like structures, suggesting the scroll-like structures of the materials were not affected by the thermal annealing process obviously.

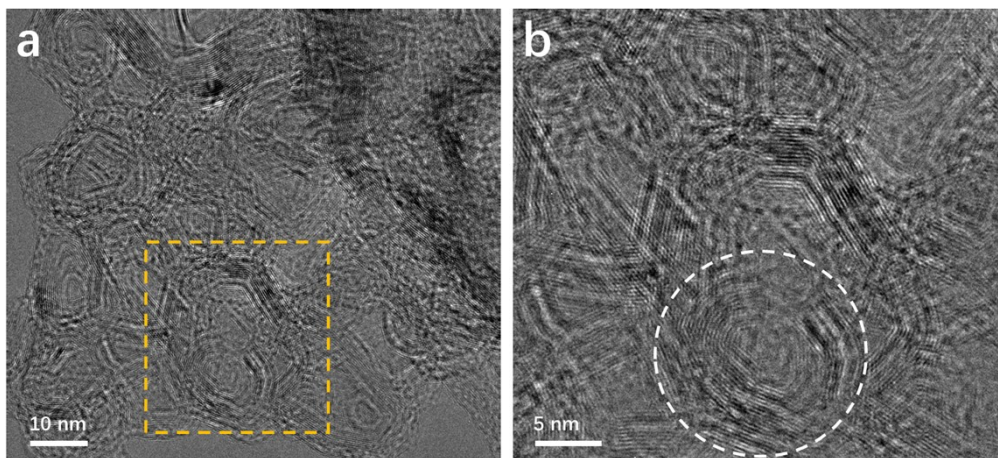


Figure S6. (a) TEM image of 2H-WSe₂ nanoscrolls. (b) Enlarged image of the region enclosed by the yellow rectangle in (a).

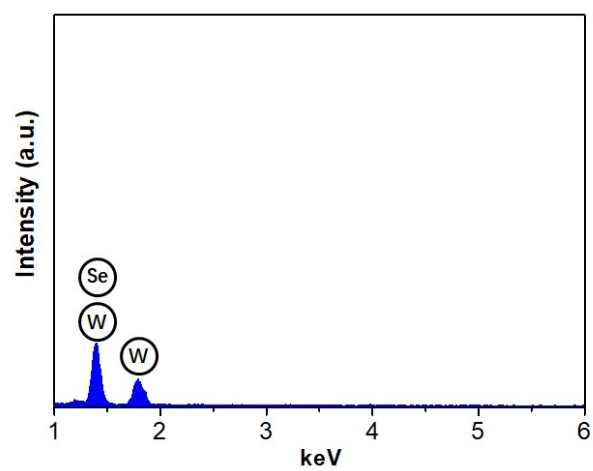


Figure S7. EDX spectrum of M-WSe₂ nanoscrolls.

The deconvolution results of the Se 3d spectrum of the M-WSe₂ nanorolls are displayed in Figure S8, which can be fitted with the metallic phase WSe₂ at about 53.7 and 54.6 eV and the 2H phase WSe₂ at about 54.7 and 55.6 eV. These results also suggest the dominant metallic phase of the sample.[2]

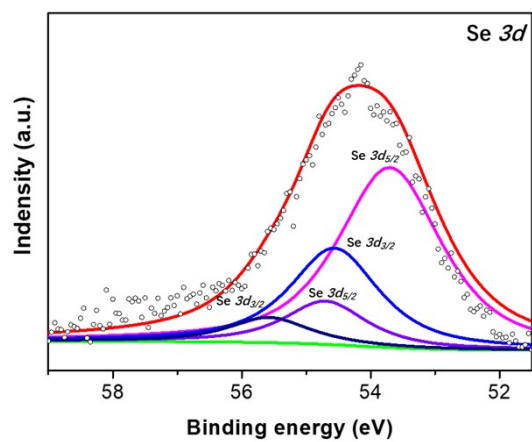


Figure S8. Se 3d XPS spectrum of the M-WSe₂ nanorolls.

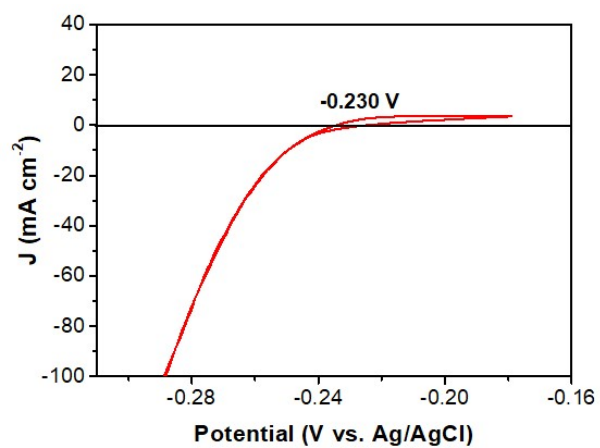


Figure S9. Cyclic voltammety curve measured at a scan rate of 1 mV s^{-1} in H_2 -saturated $0.5 \text{ M H}_2\text{SO}_4$ solution for the calibration of Ag/AgCl electrode with respect to RHE. Both the working and counter electrodes are Pt wires in the test.

To understand the origin of such high intrinsic HER activity of our as-prepared M-WSe₂ nanoscrolls, the electrochemical impedance spectroscopy (EIS) analysis was first conducted. As shown in Figure S10, the Nyquist plot of M-WSe₂ nanoscrolls shows a remarkably smaller charge transfer resistance than that of 2H WSe₂ nanoscrolls, indicating the fast charge transfer process in M-WSe₂ nanoscrolls. This should be one of the main reasons for their high HER activity. The small charge transfer resistance of nanoscrolls could be attributed to the high conductivity resulting from the unique metallic phase structure. As known, WSe₂ in the metallic phase exhibits metallic conductivity while the one in the 2H phase is a semiconductor. Moreover, the specific HER activity of M-WSe₂ and 2H WSe₂ nanoscrolls was estimated and presented in Figure S11 and Figure S12. It can be seen that, under the same applied potential, M-WSe₂ nanoscrolls exhibit a much higher specific current density than 2H WSe₂ nanoscrolls. This suggests that M-WSe₂ nanoscrolls are more intrinsically active for HER as compared with 2H WSe₂ nanoscrolls.[3, 4]

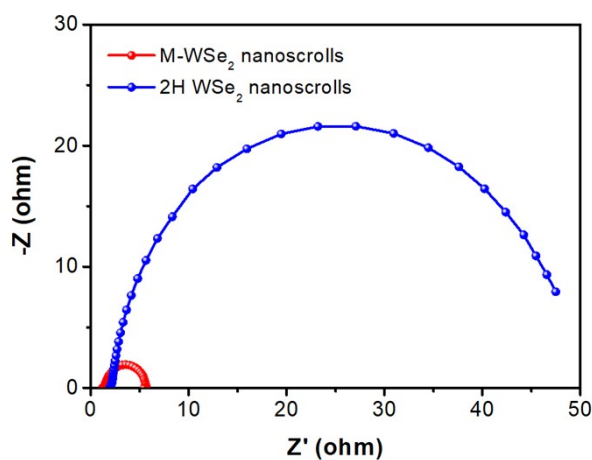


Figure S10. Electrochemical impedance spectroscopy Nyquist plots of metallic WSe₂ nanoscrolls and 2H WSe₂ nanoscrolls at the working potential of -0.282 V (vs. RHE).

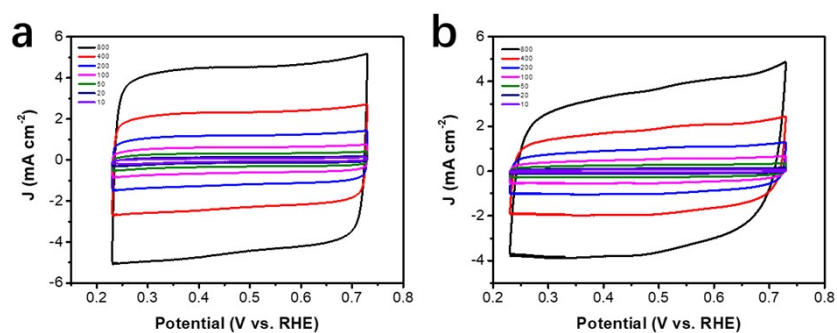


Figure S11. (a, b) Cyclic voltammograms for (a) metallic WSe₂ nanoscrolls and (b) 2H WSe₂ nanoscrolls, which were measured in a non-Faradaic region of the voltammogram at various scan rates.

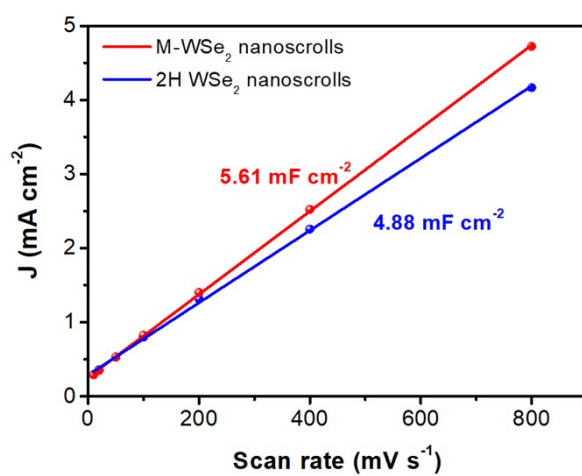


Figure S12. The ECSAs of metallic WSe₂ nanoscrolls and 2H WSe₂ nanoscrolls calculated from CVs measured at various scan rates (10-800 mV s⁻¹, Figure S11).

In addition to the good electrocatalytic activity, M-WSe₂ nanoscrolls also have excellent durability for HER. As shown in Figure S13a, the HER polarization curve of M-WSe₂ nanoscrolls measured after 10,000 sweeping cycles almost overlaps with the initial one, indicating the negligible loss in activity during the long-term test. Moreover, the chronoamperometry tests of M-WSe₂ nanoscrolls in Figure S13b also show no apparent decrease in current densities over 12 h. This further confirms the good stability of M-WSe₂ nanoscrolls for HER under acid conditions. Additionally, the cycle stability of the M-WSe₂ nanoscrolls was measured by cyclic voltammetry. As shown in Figure S14, after 10000 cycles there is no significant change in the CV curves, again indicating the good stability of M-WSe₂ nanoscrolls.

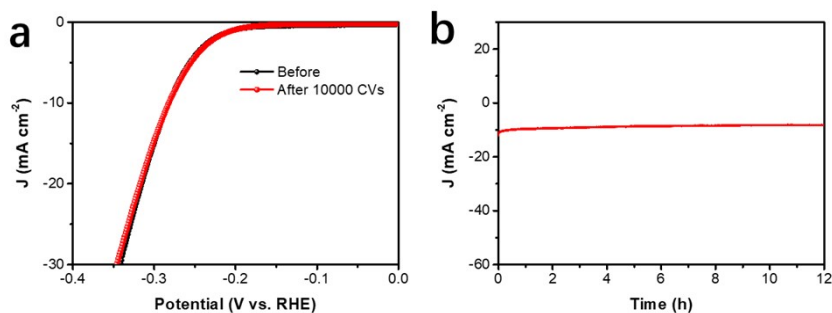


Figure S13. (a,b) Long-term stability tests for M-WSe₂ nanoscrolls. (a) The polarization curves were measured before and after 10,000 sweeping cycles in 0.5 M H₂SO₄ solution. (b) Chronoamperometric curves of M-WSe₂ nanoscrolls.

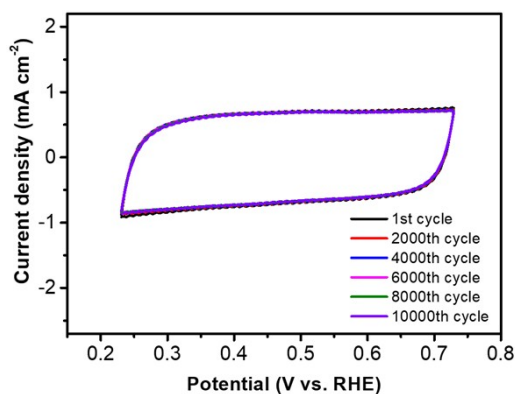


Figure S14. Cyclic voltammograms for metallic WSe₂ nanoscrolls, which were measured in a non-Faradaic region of the voltammogram at scan rates of 100mV s⁻¹.

Table S1. Electrochemical HER results for various TMDs-based HER electrocatalysts.

Electrocatalyst	Overpotential at 10 mA cm⁻² (mV)	Tafel slope (mV dec⁻¹)	Reference
WSe ₂	372	105	[5]
Spiral WS ₂	560 (vs. Ag/AgCl)	81	[6]
Monolayer WS ₂	642 (vs. Ag/AgCl)	121	[6]
WS ₂ nanosheets	310	95	[7]
Au-MoS ₂	263	71	[8]
Mn(HS)-MoS ₂	318	82	[9]
WS ₂ quantum sheets	285	116	[10]
WSe ₂ quantum sheets	331	78	[10]
WTe ₂ quantum sheets	435	162	[10]
2H WSe ₂ nanosheets	640	232	[11]
1T' WSe ₂ nanosheets	510	150	[11]
M-WSe ₂ nanoscrolls	282	82.3	This work

References

- [1] Y. Yu, G.H. Nam, Q. He, X.J. Wu, K. Zhang, Z. Yang, J. Chen, Q. Ma, M. Zhao, Z. Liu, F.R. Ran, X. Wang, H. Li, X. Huang, B. Li, Q. Xiong, Q. Zhang, Z. Liu, L. Gu, Y. Du, W. Huang, H. Zhang, High phase-purity 1T'-MoS₂- and 1T'-MoSe₂-layered crystals, *Nat. Chem.*, 10 (2018) 638-643.
- [2] N. Rohaizad, C.C. Mayorga-Martinez, Z. Sofer, M. Pumera, 1T-Phase Transition Metal Dichalcogenides (MoS₂, MoSe₂, WS₂, and WSe₂) with Fast Heterogeneous Electron Transfer: Application on Second-Generation Enzyme-Based Biosensor, *ACS Appl Mater Interfaces*, 9 (2017) 40697-40706.
- [3] Y. Huang, Y. Sun, X. Zheng, T. Aoki, B. Pattengale, J. Huang, X. He, W. Bian, S. Younan, N. Williams, J. Hu, J. Ge, N. Pu, X. Yan, X. Pan, L. Zhang, Y. Wei, J. Gu, Atomically engineering activation sites onto metallic 1T-MoS₂ catalysts for enhanced electrochemical hydrogen evolution, *Nat Commun*, 10 (2019) 982.
- [4] S. Deng, Y. Zhong, Y. Zeng, Y. Wang, Z. Yao, F. Yang, S. Lin, X. Wang, X. Lu, X. Xia, J. Tu, Directional Construction of Vertical Nitrogen-Doped 1T-2H MoSe₂/Graphene Shell/Core Nanoflake Arrays for Efficient Hydrogen Evolution Reaction, *Adv. Mater.*, 29 (2017) 1700748.
- [5] S.R. Kadam, A.N. Enyashin, L. Houben, R. Bar-Ziv, M. Bar-Sadan, Ni-WSe₂ nanostructures as efficient catalysts for electrochemical hydrogen evolution reaction (HER) in acidic and alkaline media, *J. Mater. Chem. A*, 8 (2020) 1403-1416.
- [6] P.V. Sarma, A. Kayal, C.H. Sharma, M. Thalakulam, J. Mitra, M.M. Shaijumon, Electrocatalysis on Edge-Rich Spiral WS₂ for Hydrogen Evolution, *ACS Nano*, 13 (2019) 10448-10455.
- [7] C. Tan, Z. Luo, A. Chaturvedi, Y. Cai, Y. Du, Y. Gong, Y. Huang, Z. Lai, X. Zhang, L. Zheng, X. Qi, M.H. Goh, J. Wang, S. Han, X.J. Wu, L. Gu, C. Kloc, H. Zhang, Preparation of high-percentage 1T-phase transition metal dichalcogenide nanodots for electrochemical hydrogen evolution, *Adv. Mater.*, 30 (2018) 1705509.
- [8] Y. Li, M.B. Majewski, S.M. Islam, S. Hao, A.A. Murthy, J.G. DiStefano, E.D. Hanson, Y. Xu, C. Wolverton, M.G. Kanatzidis, M.R. Wasielewski, X. Chen, V.P. Dravid, Morphological Engineering of Winged Au@MoS₂ Heterostructures for Electrocatalytic Hydrogen Evolution, *Nano Lett.*, 18 (2018) 7104-7110.
- [9] Z. Cai, T. Shen, Q. Zhu, S. Feng, Q. Yu, J. Liu, L. Tang, Y. Zhao, J. Wang, B. Liu, H.M. Cheng, Dual-Additive Assisted Chemical Vapor Deposition for the Growth of Mn-Doped 2D MoS₂ with Tunable Electronic Properties, *Small*, 16 (2020) e1903181.
- [10] Z. Chen, Y. Li, K. Wang, Y. Zhang, Scalable production of intrinsic WX₂(X = S, Se, Te) quantum sheets for efficient hydrogen evolution electrocatalysis, *Nanotechnology*, 32 (2021).
- [11] M.S. Sokolikova, P.C. Sherrell, P. Palczynski, V.L. Bemmer, C. Mattevi, Direct solution-phase synthesis of 1T' WSe₂ nanosheets, *Nat. Commun.*, 10 (2019).